### Title

Predictable and unpredictable deviance detection in the human hippocampus and amygdala.




### Journal

Cerebral Cortex, 34(2)



### Authors

Tzovara, Athina

Fedele, Tommaso

Sarnthein, Johannes

et al.



### Publication Date

2024-01-31

### DOI

10.1093/cercor/bhad532

Peer reviewed

OXFORD

*Cerebral Cortex*, 2024, **34**, 1–12
https://doi.org/10.1093/cercor/bhad532
Advance access publication date 12 January 2024
**Original Article**

# Predictable and unpredictable deviance detection in the human hippocampus and amygdala

Athina Tzovara[1,2,3,*], Tommaso Fedele[4], Johannes Sarnthein[4], Debora Ledergerber[5], Jack J. Lin[6,7], Robert T. Knight[1,8]

[1]Helen Wills Neuroscience Institute, University of California, 450 Li Ka Shing Biomedical Center, Berkeley, CA 94720-3370, United States,
[2]Institute of Computer Science, University of Bern, Bern, Neubrückstrasse 3012, Switzerland,
[3]Center for Experimental Neurology - Sleep Wake Epilepsy Center | NeuroTec, Department of Neurology, Inselspital, Bern University Hospital, University of Bern, Bern, Freiburgstrasse 3010, Switzerland,
[4]Neurosurgery Department, University Hospital Zürich, Zürich, Frauenklinikstrasse 8091, Switzerland,
[5]Swiss Epilepsy Center, Klinik Lengg, Zürich, Bleulerstrasse 8008, Switzerland,
[6]Department of Neurology, University of California, Davis, Folsom Boulevard, Davis, CA 95816, USA,
[7]The Center of Mind and Brain, University of California, Davis, Cousteau Pl, Davis, CA 95618, USA,
[8]Department of Psychology, University of California, Berkeley, CA 94720-1650, USA

[*]Corresponding author: Institute of Computer Science, University of Bern, Neubrückstrasse 10, CH3012 Bern, Switzerland. Email: athina.tzovara@unibe.ch

Our brains extract structure from the environment and form predictions given past experience. Predictive circuits have been identified in wide-spread cortical regions. However, the contribution of medial temporal structures in predictions remains under-explored. The hippocampus underlies sequence detection and is sensitive to novel stimuli, sufficient to gain access to memory, while the amygdala to novelty. Yet, their electrophysiological profiles in detecting predictable and unpredictable deviant auditory events remain unknown. Here, we hypothesized that the hippocampus would be sensitive to predictability, while the amygdala to unexpected deviance. We presented epileptic patients undergoing presurgical monitoring with standard and deviant sounds, in predictable or unpredictable contexts. Onsets of auditory responses and unpredictable deviance effects were detected earlier in the temporal cortex compared with the amygdala and hippocampus. Deviance effects in 1–20 Hz local field potentials were detected in the lateral temporal cortex, irrespective of predictability. The amygdala showed stronger deviance in the unpredictable context. Low-frequency deviance responses in the hippocampus (1–8 Hz) were observed in the predictable but not in the unpredictable context. Our results reveal a distributed network underlying the generation of auditory predictions and suggest that the neural basis of sensory predictions and prediction error signals needs to be extended.

*Key words*: amygdala; auditory predictions; deviance; hippocampus; intracranial EEG.

## Introduction

The human brain has an astonishing capacity in detecting patterns from the environment in a quick and automatic way (Bar 2009). Detecting patterns in sensory stimuli allows making predictions about future events before they occur, based on current sensory input (Heilbron and Chait 2018). Every time that a pattern is violated, an internal model of the world is updated through prediction error signals, which quantify the difference between expected and received outcome (Heilbron and Chait 2018). One experimental testbed for studying sensory predictions is through auditory deviance paradigms. These paradigms comprise of series of commonly repeated (standard) sounds, which are occasionally replaced by deviant tones (Garrido et al. 2009; Tivadar et al. 2021).

Because of the difficulty in assessing electrophysiological activity in subcortical regions in a noninvasive way, the search for a sensory predictive network in the auditory modality has mainly focused on a two-node circuit, including mainly the temporal lobe and prefrontal areas (Garrido et al. 2009; Dürschmid et al. 2018, 2016; Rosburg et al. 2005; Canolty et al. 2006; Phillips et al. 2016). The most prevalent view is that sensory areas compute a low-level predictive signal, comparing current sensory input to the immediate past and detect violations of auditory sequences (Dürschmid et al. 2016). This two-node temporal-to-prefrontal circuit underlying sensory predictions has been well characterized by noninvasive (Garrido et al. 2008; Chennu et al. 2013) and invasive electrophysiology (Rosburg et al. 2005; Dürschmid et al. 2016; Phillips et al. 2016; Edwards et al. 2005), establishing a cortical hierarchy of auditory predictions.

Beyond this cortical two-node network, additional brain regions have sensitivity to sensory predictions and deviance, including the insula (Blenkmann et al. 2019), nucleus accumbens (Dürschmid et al. 2016), and also the hippocampus and amygdala (Halgren et al. 1980; Knight 1996). Although recent studies have specifically targeted some of these regions, such as the nucleus accumbens (Dürschmid et al. 2016), or the insula (Blenkmann et al. 2019), in relation to deviance detection, the role of the hippocampus and amygdala in forming auditory predictions is by comparison under-explored.

Both the hippocampus and amygdala are sensitive to auditory stimuli (Cusinato et al. 2023) and infrequent auditory events (Halgren et al. 1980; Knight 1996), but their specific role in the formation of auditory predictions remains unclear, as well as their integration with other cortical areas (Johnson et al. 2020). Previous studies based on functional Magnetic Resonance Imaging (fMRI) or magnetoencephalography (MEG) have shown that the hippocampus is sensitive to violations of expected events

**Received:** November 18, 2022. **Revised:** December 15, 2023. **Accepted:** December 16, 2023

(Kumaran and Maguire 2006; Chen et al. 2013; Garrido et al. 2015), mainly through low-frequency oscillations (Garrido et al. 2015; Recasens et al. 2018). Intriguingly, the hippocampus is also sensitive to unexpected visual events (Axmacher et al. 2010), memory functions (Johnson and Knight 2015), visual regularities (Schapiro et al. 2012; Ekman et al. 2023), and linguistic stimuli (Jafarpour et al. 2017) possibly arbitrating between predictions and encoding of memories (Sherman and Turk-Browne 2020).

The amygdala is also sensitive to unexpected novel events (Blackford et al. 2010; Balderston et al. 2013) and to violations of expected auditory input (James et al. 2012). Interestingly, invasive electrophysiology recordings in macaques showed that single unit activity in the amygdala is sensitive to deviant auditory stimuli, with comparable latencies to those of prefrontal neurons (Camalier et al. 2019). These studies suggest that, contrary to the hippocampus, which is primarily sensitive to regular events and sequences, the amygdala may be more fine-tuned in the detection of unexpected deviance. Indeed, the hippocampus has been long targeted as a key region underlying sequence learning (Eichenbaum 2013), and formation of predictions (Lisman and Redish 2009), which imply increased sensitivity to expected events. In addition, the hippocampus is also sensitive to highly novel stimuli that may be salient for memory storage (Knight 1996; Jafarpour et al. 2017). In contrast, the amygdala is mostly known as a structure underlying detection of novelty (Blackford et al. 2010), which by extension implies sensitivity to unexpected acoustic events. Despite ample evidence for the involvement of the hippocampus and amygdala in detecting violations of environmental regularities, the specific function of each region in detecting deviant inputs and prediction remains underexplored.

Here, we aimed at shedding light on the role of the hippocampus and amygdala in detecting violations of auditory rules, and contrasting that to the well-established role of the temporal cortex (Dürschmid et al. 2016; Rosburg et al. 2005; Edwards et al. 2005). We hypothesized that in addition to a cortical mechanism for detection of auditory events and deviant auditory events, there also exists medial temporal lobe contributions from the hippocampus and amygdala. To dissociate effects of deviance and predictability, we used a paradigm comprising of standard and deviant sounds, presented in a temporally predictable or unpredictable way (Dürschmid et al. 2016). We recorded intracranial electroencephalography (iEEG) in patients with epilepsy to directly assess neural activity of the hippocampus and amygdala. We provide evidence for a distributed temporal lobe network underlying the generation of auditory predictions and highlight the role of the hippocampus and amygdala in detecting auditory rules and their violations.

# Materials and methods

## Patients

We recorded intracranial EEG data in eight patients with pharmacoresistant epilepsy (mean age: 29 years, 3 women), undergoing presurgical monitoring. All patients had implanted depth electrodes, targeting the hippocampus and amygdala, among other regions (Table 1 for an overview of electrodes across patients). Patients were selected on the basis of having electrode coverage in the mesio-temporal lobe from at least one seizure-free hemisphere. Recordings took place at the University of California Irvine Medical Center, United States, the University of Zurich (implantation), and the Swiss Epilepsy Center in Zurich (recordings), Switzerland. Patients gave written informed consent to participate in this study, approved by institutional ethics review boards of the University Hospital of Zurich (PB 2016–02055), UC Berkeley, and UC Irvine. All experiments were performed in accordance with the 6th Declaration of Helsinki.

## Paradigm

Patients were presented with series of standard (80%) and deviant (20%) sounds during wakefulness. Sounds were pure tones, lasting 100 ms. The standard sounds' pitch was drawn from a gaussian distribution with $\mu = 500$ Hz, $\sigma 2 = 125$ Hz. The pitch for deviant sounds was at the tail of the distribution with a frequency of 2,000 Hz. Deviant sounds were presented in a temporally predictable (after 4 standards) or unpredictable (after 3–8 standards) context (Fig. 1). Distribution of standard sounds between consecutive deviants differed between predictable and unpredictable sequences following a previously published study (Dürschmid et al. 2016), as opposed to other protocols that control for the shape of this distribution (Lecaignard et al. 2015). The sound-to-sound interval (stimulus onset asynchrony) was 600 ms. Sounds were presented in two blocks of 500 trials, one for the predictable and one for the unpredictable context, lasting ~5′ each. Two additional blocks were recorded, in which the pitch of the standard sounds was drawn from a distribution with high variance, but were not analyzed, as they were out of the scope of the present study. The order of blocks was randomized for each patient. Patients were instructed to watch a silent video and ignore the sounds.

## Electrode localization

Electrodes were localized using merged postoperative computed tomography (CT) and preoperative structural $T_1$-weighted MRI scans. The CT scan was registered to the preoperative MRIs, using a standard electrode localization procedure, implemented in Fieldtrip (Stolk et al. 2018). The electrode locations were visualized for each patient in native space, and their location was identified by a neurologist. To visualize the electrode locations across the group of patients, the aligned electrodes were warped onto a template brain in MNI space. We considered the most consistent localizations of contacts across all patients and retained for further analysis temporal lobe electrodes which were localized in three different subregions (hippocampus/amygdala/temporal cortex/ TC, spanning along the superior temporal sulcus-areas, Table 1). We retained electrodes belonging to one of these regions that were not part of a seizure onset zone or other artifacts. The total number of retained electrodes per patient is shown in Table 1, and their spatial coverage in Fig. 5.

## Acquisition and preprocessing of electrophysiological data

Intracranial EEG was recorded over arrays of depth electrodes, typically consisting of eight stainless contacts each (AD-Tech, electrode diameter: 3 mm, intercontact spacing: 10 mm). All data were visually inspected by a neurologist (RTK) to (i) exclude electrodes that were within the seizure onset zone and (ii) exclude periods of epileptic activity in the remaining electrodes. Continuous data were notch filtered, down-sampled to 500 Hz, and re-referenced to a bipolar montage, according to their nearest neighbor on the same depth, to remove any source of noise from the common reference signal, following recommendations in the analysis of iEEG data (Lachaux et al. 2012; Mercier et al. 2022). Signals at all electrodes were band-pass filtered between 0.1 and 20 Hz prior to the extraction of local field event related potentials.

Peri-stimulus epochs were then extracted, spanning from −100 ms before the sounds' onset to 500-ms poststimulus onset.

**Table 1.** Description of patients and electrode locations. For each patient, we display the total number of electrodes that were located in each of our regions of interest (column total) and the number of electrodes that were responsive to auditory stimuli (column responsive). Only electrodes that were located in seizure free regions are included.

| Patient | Age | Sex | Amygdalar electrodes | | Hippocampal electrodes | | Superior temporal electrodes | |
|---|---|---|---|---|---|---|---|---|
| | | | Total | Responsive | Total | Responsive | Total | Responsive |
| 1 | 24 | F | 5 | 0 | 5 | 3 | 4 | 2 |
| 2 | 28 | M | 6 | 2 | 3 | 2 | 5 | 4 |
| 3 | 20 | F | 3 | 2 | 0 | 0 | 4 | 2 |
| 4 | 28 | M | 4 | 1 | 7 | 3 | 13 | 8 |
| 5 | 57 | M | 3 | 1 | 4 | 2 | 4 | 3 |
| 6 | 29 | M | 3 | 0 | 5 | 1 | 0 | 0 |
| 7 | 26 | M | 4 | 3 | 11 | 3 | 14 | 14 |
| 8 | 21 | F | 5 | 3 | 3 | 1 | 7 | 6 |
| Total | - | - | 33 | 12 | 38 | 15 | 51 | 39 |

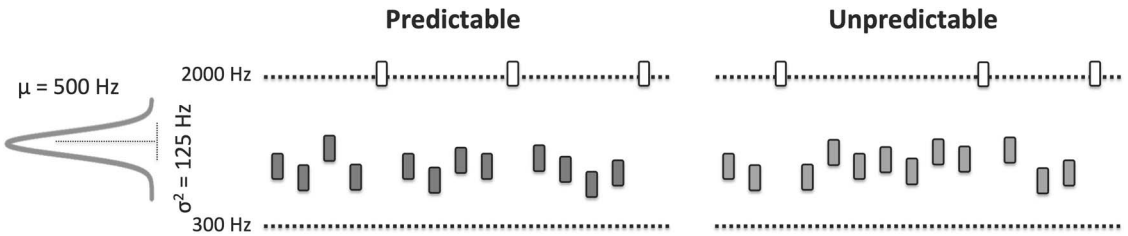


**Fig. 1.** Task design. Patients were presented with series of standard (80%, gray) and deviant (20%, white) sounds. The standard sounds' pitch was drawn from a gaussian distribution with $\mu = 500$ Hz, $\sigma^2 = 125$ Hz. Deviant sounds laid at the tail of the distribution with a frequency of 2,000 Hz. Deviant sounds were presented in a temporally predictable (after 4 standards) or unpredictable (after 3–8 standards) context.

All epochs were then visually inspected to exclude any remaining artifacts. Data processing was performed using MNE python (Gramfort et al. 2013).

## Responsive electrodes

We focused all analyses on electrodes that responded to the auditory stimulation. To not bias our search for deviance and predictability effects, we pulled all cleaned epochs together and sought electrodes that responded to all sounds irrespective of the sounds' identity.

For each electrode, we contrasted the time-point by-time poststimulus local field potentials with baseline prestimulus activity (−100 to 0 ms), using *t*-tests. For this, we pooled together all available baselines for a given electrode, across trials, and randomly sampled the equivalent of 100 ms from this pool. This was repeated with 500 iterations, to obtain a distribution of available baselines, which were then used to baseline correct each trial. This approach is advantageous for selecting responsive electrodes and is commonly used in the field of iEEG research (Blenkmann et al. 2019; Kam et al. 2019), as it is less likely to be affected by isolated baseline fluctuations, as statistical tests for responsiveness are performed at the single-trial level.

The resulting *t*-values were corrected for multiple comparisons based on the false discovery rate ($P < 0.05$). Onsets of responsiveness were defined at the single electrode level, by considering the first time point that showed a significant response. Peaks of responsiveness were considered by considering the location of the maximum absolute value among all significant *t*-values. Onset and peak latencies were contrasted at the group level, pulling all electrodes together across regions using linear mixed effect models, with a random intercept of patient to account for across patient differences.

## Deviance effects

Deviance effects were parametrized by *F*-values, which were computed for each electrode, and context based on a one-way ANOVA, with a factor of deviance, as in a previous studies using similar paradigms (Kam et al. 2021; Dürschmid et al. 2016). Onsets of deviance effects for each context were defined as the first time-point where significance was reached, assessed by comparing the true values to the distribution of effects obtained via 1,000 random permutations in the labels of standard and deviant epochs (Dürschmid et al. 2016). These were then contrasted with a linear mixed effects model with a factor of region, a factor of context (predictable unpredictable), and their interaction, as well as a random factor of patient. Group-level effects of predictability were identified by further contrasting the time-courses of *F*-values quantifying deviance effects for the predicable and unpredictable contexts, as in previous studies using a similar paradigm (Dürschmid et al. 2016). This approach is equivalent to a 2 by 2 ANOVA and was preferred over a "classical" implementation of a 2-factorial test, because of the bipolar reference in the data. All electrodes were rereferenced to their neighbors, a positive peak in one pair could deflect as a negative peak in the next, resulting in a close to zero on average. By parametrizing LFPs with *F*-values, the sign of LFP measures becomes irrelevant, and only information about the magnitude of effects is retained, making it possible to perform group-level analyses.

## Time–frequency analysis

For each responsive channel, we decomposed the time course of LFPs in time–frequency representations, using Morlet wavelets with multitaper windows (function tfr_array_multitaper from MNE), applied with 0.5-Hz steps, from 1 to 20 Hz. The time–frequency decomposition was performed for each single trial. The resulting single-trial power was normalized by the log-ratio

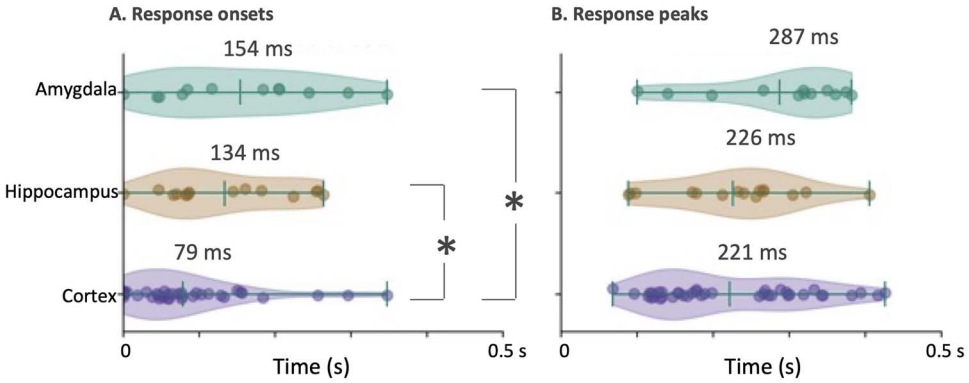


**Fig. 2.** Onsets and peaks for responsive amygdalar, hippocampal, and cortical electrodes in LF-ERPs (1–20 Hz). Responsiveness was assessed by merging responses to all sound categories. Responsive electrodes in the cortex showed a significantly earlier onset compared with hippocampal and amygdalar ones ($F(1,45) = 4.06$, $P < 0.05$ for cortex vs. hippocampus and $F(1,43) = 8.08$, $P < 0.05$ for cortex vs. amygdala).

of the prestimulus baseline. Single-trial power was then averaged within experimental conditions.

### Statistical contrasts

Statistical tests grouping data from multiple patients, for example testing for response onsets, were based on linear mixed effects models, with a random intercept for accounting for different patients, as it is common practice in the field (Cusinato et al. 2023; Johnson et al. 2018). Bonferroni correction was used for correcting for multiple comparisons. For statistical tests performed in time–frequency analyses of iEEG signals, correction for multiple comparisons was achieved via cluster-based permutation tests ($P < 0.05$, 1,000 permutations).

## Results

Patients were presented with series of standard and deviant sounds (80% and 20% of the time, respectively). Deviant sounds were presented in a temporally predictable (i.e. always after four standard sounds) or unpredictable (after 3–8 standard sounds) context (Fig. 1). Patients were instructed to focus their attention to a silent movie and ignore the presented sounds.

### Responsive electrodes

We first assessed electrodes that were responsive to all sounds, irrespective of context and deviance manipulations, by testing for significant changes in 1–20 Hz local field event-related potentials (LF-ERPs) with respect to a 100-ms baseline period. Patients had consistent electrode implantations in the lateral and medial temporal lobe, covering the lateral temporal cortex and the hippocampus and amygdala (Table 1 for electrode coverage per patient and region). All three regions contained responsive electrodes to sounds across patients (Table 1). Electrodes in the temporal cortex showed a significantly earlier response onset than electrodes in the amygdala (Fig. 2A, $F(1,43) = 8.08$, $P < 0.05$, linear mixed effects models accounting for different patients here and in the following), and an earlier response than electrodes in the hippocampus ($F(1,45) = 4.06$, $P < 0.05$). The mean response onset across patients and electrodes was at 79 ms for the temporal cortex, 134 ms for the hippocampus, and 154 ms for the amygdala (Fig. 2A). There was no significant difference between the onsets of the hippocampus and amygdala ($F(1,18) = 0.12$, $P = 0.74$). Response peaks showed a similar tendency as onsets, with peak responses occurring at 221 ms on average for temporal electrodes, and at 226 ms for hippocampal and 287 ms for amygdalar ones (Fig. 2B).

### Deviance effects

Focusing on responsive electrodes, we then contrasted local field event-related potentials (LF-ERPs) in response to standard vs. deviant sounds. As expected from previous studies (Dürschmid et al. 2016), these showed a strong deviance response in temporal areas (Fig. 3 for exemplar LF-ERPs) and deviance responses for both the predictable and unpredictable contexts (Fig. 3C and D for exemplar responses). The deviance effects in amygdala and hippocampus are shown in Fig. 4. To quantify these responses at the group level, we parametrized LF-ERPs in response to standard vs. deviant sounds for each context, by *F*-values. These quantify the strength of differential responses to standard vs. deviant sounds (Fig. 5A for *F*-values, and Supplemental Fig. 3 for the corresponding omega squared values which are not biased by sample size). Please note that group level results in Fig. 5 are visualized via *F*-values similar to previous studies (Dürschmid et al. 2016), and not as LF-ERPs. Because a bipolar reference was used in the analysis, neighbor electrodes can have responses of opposing sign, and therefore, averaging all LF-ERPs is not meaningful. *F*-values overcome this issue, as they quantify the strength of deviance effects across trials, irrespective of the sign of LF-ERPs responses.

At the group level, the temporal cortex showed the strongest *F*-values for both predictable and unpredictable contexts (Fig. 5A, purple plots). However, there was no significant difference in the *F*-values between the two contexts.

The hippocampus showed deviance responses in the LF-ERP range for both contexts (Fig. 4A for exemplar LF-ERPs in the hippocampus). At the group level, we observed a significantly stronger deviance response for the predictable context compared with the unpredictable one (Fig. 5A, for group results quantified via *F*-values, black marks on *x*-axis denote significant differences between predictable and unpredictable contexts). For the predictable context in particular, deviance *F*-values were strong early in time and even before the sounds' onset, which can be explained by the fact that the sequence, and the occurrence of a deviant sound can be fully predicted (Schapiro et al. 2012; Jafarpour et al. 2017). In the amygdala by contrast, the strongest deviance effects were observed for the unpredictable context, and at late latencies, ~300-ms poststimulus onset (Fig. 5A for group *F*-values, Fig. 4B for exemplar LF-ERPs). This analysis was repeated when excluding the first standard sound after a deviant (Supplemental Fig. 1) and when quantifying deviance effects separately for each standard sound in the sequence (Supplemental Fig. 2).

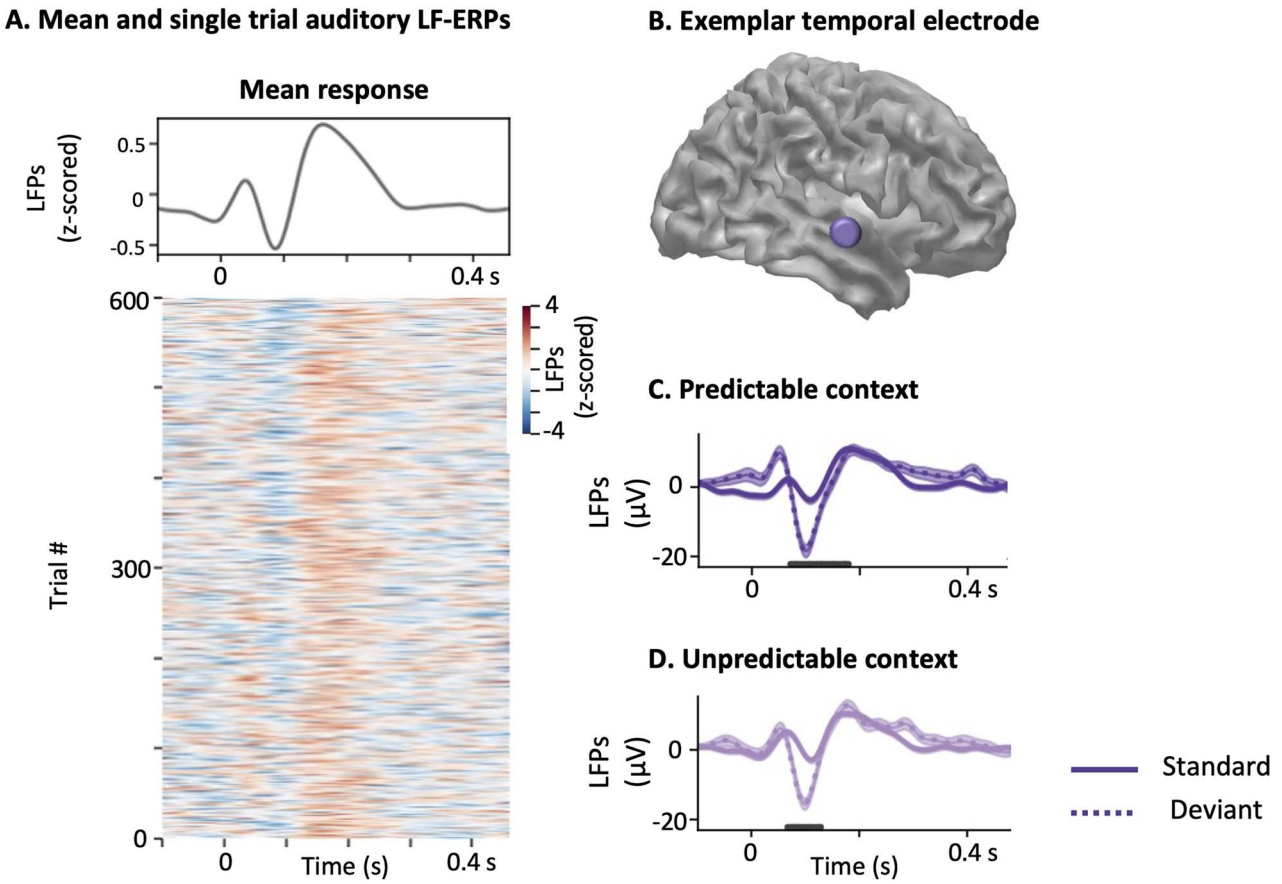


**Fig. 3.** Exemplar LF-ERPs in the temporal cortex. (A) Mean and single trial LF-ERPs for an exemplar electrode in the temporal cortex. (B) Location of this electrode with MNI coordinates: −56.79, −16.11, −4.90. (C and D) Responses to standard (full) vs. deviant (dotted lines) sounds for the predictable (C) and unpredictable (D) contexts. Horizontal lines highlight periods of significant difference between standard and deviant responses.

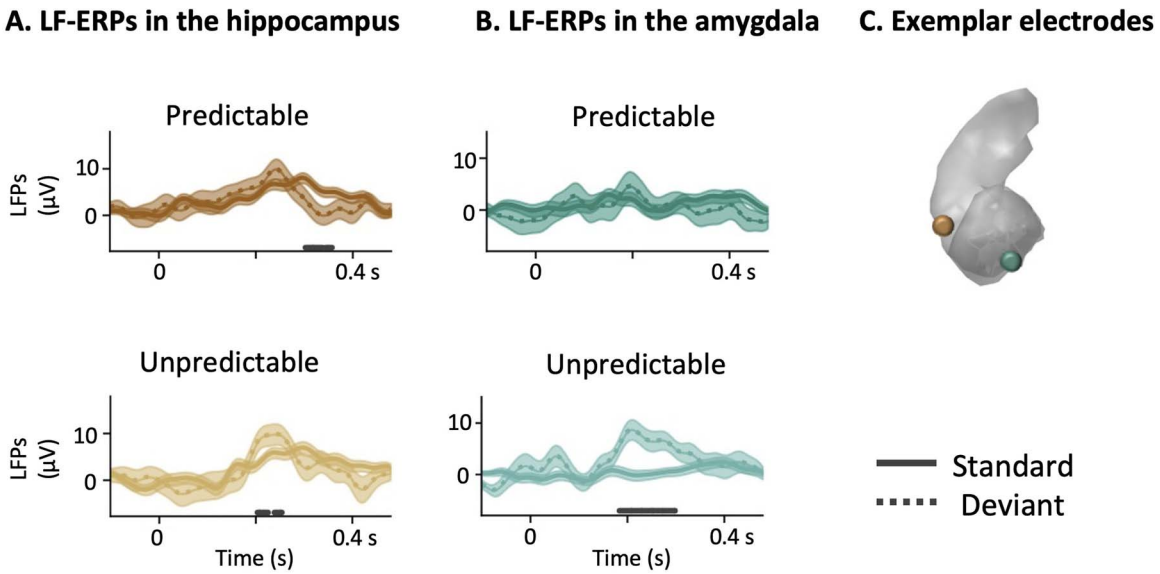


**Fig. 4.** LF-ERPs in the hippocampus (A) and amygdala (B). Top rows represent 1–20 Hz LF-ERPs in response to predictable and bottom rows to unpredictable standard and deviant stimuli. Full lines show responses to standard and dotted to deviant sounds. Horizontal lines highlight periods of significant difference. Although the hippocampus showed a deviance response both for predictable and unpredictable contexts, the amygdala showed a deviance response for the unpredictable context only. Horizontal lines highlight periods of significant deviance effects, assessed through permutation statistics. (C) Location of this contact, MNI coordinates: [37.51, −12.92, −19.24] for the hippocampus and [−21.99, −1.19, −24.26] for the amygdala.

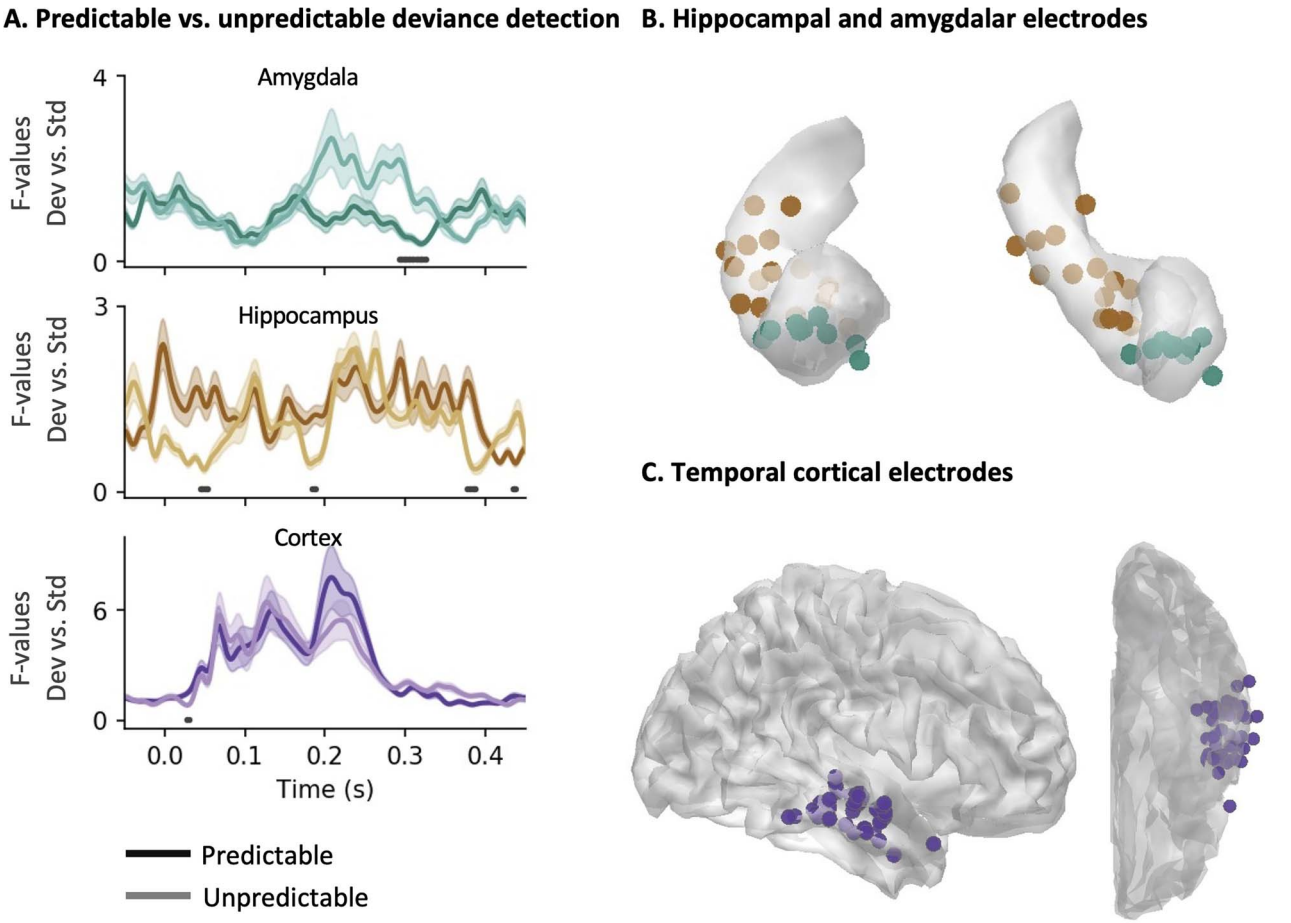


**Fig. 5.** Group level predictable and unpredictable deviance detection. (A) Time-course of F-values contrasting responses to standard vs. deviant sounds for predictable (dark lines) and unpredictable (light lines) contexts across contacts and patients. Panel (A) shows F-values, computed by contrasting LF-ERPs in response to standard vs. deviant sounds at the single-trial level, similar to previous studies (Dürschmid et al. 2016). The amygdala (top row) showed stronger F-values for the unpredictable context compared with predictable one, while the hippocampus for the predictable context. In contrast, F-values in the cortex did not differ between the two contexts. Horizontal black lines highlight periods of significant difference in F-values for predictable vs. unpredictable contexts. Please note that this figure does not quantify the timing of significant deviancy events; these are instead displayed in Fig. 6. (B and C) Overview of all electrodes for hippocampus, amygdala (B) and cortex (C), projected on MNI templates.

## Latencies of deviancy effects

After evaluating whether LF-ERP responses to standard vs. deviant sounds within each region of interest are modulated by predictability, we characterized their latency of deviance responses for each of the two contexts separately, at the level of single electrodes (Fig. 6). These latencies refer to the onset of deviance responses, i.e. differences between standard and deviant sounds in the two contexts, and not to the latency of an auditory–sensory–response (which is shown in Fig. 2). We found a significant main effect of region ($F(1, 100) = 7.95$, $P < 0.01$) and a region by predictability interaction ($F(1, 100) = 5.20$, $P = 0.02$) in the onsets of deviance effects. The main effect of predictability was not significant ($F(1, 100) = 2.17$, $P = 0.14$).

In the unpredictable context, the temporal cortex showed the earliest deviance effects, with a mean onset across patients and contacts of 100 ms (Fig. 6, light colors). Deviance effects in the hippocampus had mean onset at 210 ms (Fig. 6, light colors), significantly later than the temporal cortex ($F(1,39) = 12.83$, $P_{corr} < 0.01$). In the amygdala, unpredictable deviance had a mean onset at 195 ms, which was not significantly later than the temporal cortex when correcting for multiple comparisons ($F(1,36) = 7.61$, $P_{corr} = 0.055$).

For the predictable context, the temporal cortex had shorter latencies (105-ms poststimulus onset) than the hippocampus (121 ms) and amygdala (132 ms), but these were not significantly different (Fig. 6, dark plots).

Deviancy onset effects in the hippocampus were shorter for the predictable (121 ms) compared with the unpredictable (210 ms) contexts, but this difference was not statistically significant when correcting for multiple comparisons ($F(1,18) = 4.17$, $P_{corr} = 0.17$, Fig. 6).

## Frequency contents of deviance responses

We next evaluated the frequency content of local field potential responses to the auditory stimuli, by computing time–frequency analyses for the three regions of interest at the group level (Fig. 7). Time–frequency decompositions were computed for each single trial and averaged across trials, per electrode. These revealed a significant effect of deviance only in the hippocampus (Fig. 7). Low-frequency power, in the range of 1–8 Hz, was significantly stronger in response to deviant compared with standard sounds in the hippocampus, for the predictable context only, for a sustained period starting around 100-ms poststimulus onset (Fig. 7, gray outline highlighting a significant cluster, with a cluster-level $P_{corr} < 0.05$). Higher low-frequency power for deviant sounds

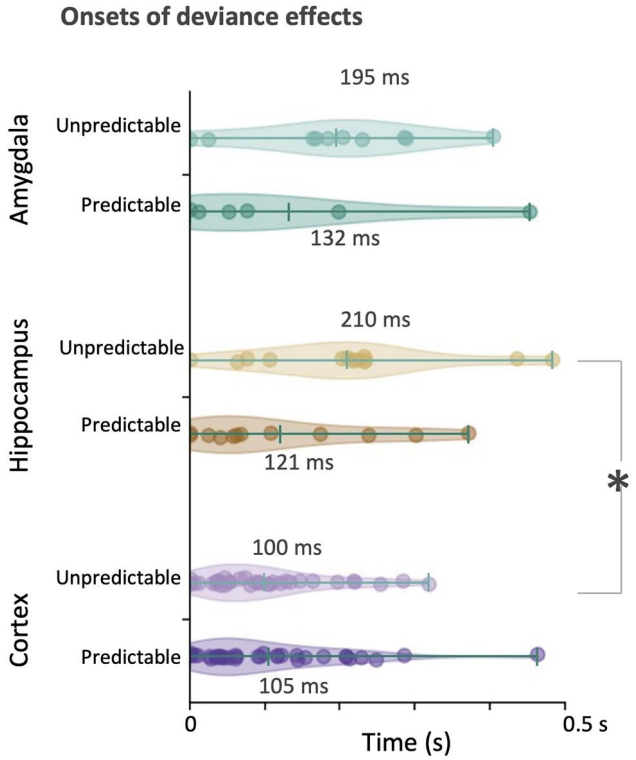


**Fig. 6.** Onsets of deviance effects in LF-ERPs for individual contacts split by context. For the unpredictable context, the onsets of deviance effects occurred at earlier latencies for temporal compared with hippocampal electrodes ($F(1,39) = 12.83$, $P_{corr} < 0.01$). No difference was observed for the predictable context.

compared with standards was observed for all patients for the predictable, but not unpredictable context (Supplemental Fig. 4). In the cortex and amygdala, there was a tendency for higher power in response to deviant sounds, but this was not significant after correcting for multiple comparisons.

## Low-frequency activity in the hippocampus supports auditory predictions

Thus far, we considered all standard sounds as one condition, irrespective of their temporal order of appearance. Next, we evaluated the link between low-frequency activity in the hippocampus and auditory predictions. We focused on the frequency range that showed a deviance effect for the predictable context in the hippocampus (Fig. 7) and we used it as mask to compute the average hippocampal power as a sequence unfolds. For this analysis, we split standard sounds into subgroups, according to their order of presentation (Fig. 8, S1–S4).

We observed a significant effect of sequence in the difference of low-frequency hippocampal power between predictable and unpredictable contexts ($F(1,14) = 7.87$, $P_{corr} < 0.05$, Fig. 8B). This was driven by a difference in low-frequency activity between the deviant and four standard tones (Fig. 8C, $F(1,14) = 8.29$, $P_{corr} < 0.05$). Post-hoc analysis revealed a significant difference between low-frequency power in response to the deviant sound and the second or fourth standard sound in the sequence ($P < 0.01$, Fig. 8C, S2 vs. D and S4 vs. D). There was a trend for lower power between the third standard sound and the deviant but this was not significant ($P = 0.07$, Fig. 8C, S3 vs. D). Control analysis for the unpredictable context showed no effect of sequence (Fig. 8D, $F(1,14) = 1.27$, $P = 0.26$).

Last, we also assessed changes in hippocampal power over time as the sequence unfolds. We computed power in at 1–8 Hz (Fig. 8A). The analysis of the hippocampal power over time revealed a significant main effect of context between 0.114- and 0.170-s poststimulus onset, but neither main effect of sequence order nor interaction. Moreover, 1–8 Hz power in the hippocampus was modulated by the order of sound presentation between 232 and 290 ms, and between 318 and 414 ms postsound onset (Fig. 8A, horizontal lines, $F(1,14) = 7.7.00$, $P < 0.01$ at 260 ms). As a control analysis, there was no power modulation by auditory sequence neither in the amygdala ($F < 3.01$, $P > 0.09$), nor the temporal cortex ($F < 5.2$, $P > 0.06$; Supplemental Fig. 5).

# Discussion

Intracranial EEG recordings in humans provided direct evidence of medial temporal lobe contributions in the formation of auditory predictions. We found that the hippocampus and amygdala are sensitive to deviant sounds with distinct roles. Deviance effects in LF-ERPs in the hippocampus were stronger for the predictable compared with the unpredictable context, with an opposite pattern in the amygdala showing enhanced responses for unpredictable deviance. In contrast, deviance effects in the temporal cortex were not modulated by predictability, in accordance to previous reports using a similar paradigm in a different group of patients (Dürschmid et al. 2016). Taken together, our findings suggest the existence of a distributed network in the medial temporal lobe underlying sensory predictions: while the temporal cortex computes "low" level predictions, comparing each sensory input to the immediate past, the hippocampus maintains a longer memory trace of auditory patterns, spanning over sequences of sounds, and is particularly active when a violation of the sequence can be predicted.

## Mesio-temporal network underlying auditory predictions

Our findings expand the network of deviance detection beyond a two-node cortical network, which has been excessively studied using mainly noninvasive imaging (Garrido et al. 2009; Chennu et al. 2013). Invasive EEG recordings have been used to confirm this two-node network (Dürschmid et al. 2016; Phillips et al. 2016), and have also demonstrated additional regions sensitive to deviance, including the insula (Blenkmann et al. 2019), the nucleus accumbens (Dürschmid et al. 2016), the hippocampus, and the amygdala (Halgren et al. 1980; Camalier et al. 2019). Here, we focused on the hippocampus and amygdala and showed that the latencies of processing deviant sounds in the amygdala follow that of the hippocampus and temporal cortex, suggesting a temporal lobe hierarchy in detecting auditory deviance. The fact that the amygdala responds to deviance at later latencies than the temporal cortex is in accordance with a recent monkey study using single unit activity (Camalier et al. 2019). Moreover, the hierarchy in auditory response latency observed in this study irrespective of deviance effects fits the latencies of auditory responses reported in a recent study using a different auditory paradigm and patients, where the temporal cortex showed earlier responses compared with both the hippocampus and amygdala (Cusinato et al. 2023).

Our results showed that on average, electrodes in the temporal cortex had the strongest deviance effect, but not a group-level predictability effect. This finding is in accord with a recent study using a similar design as ours (Dürschmid et al. 2016), which showed strong deviance but no predictability effects in

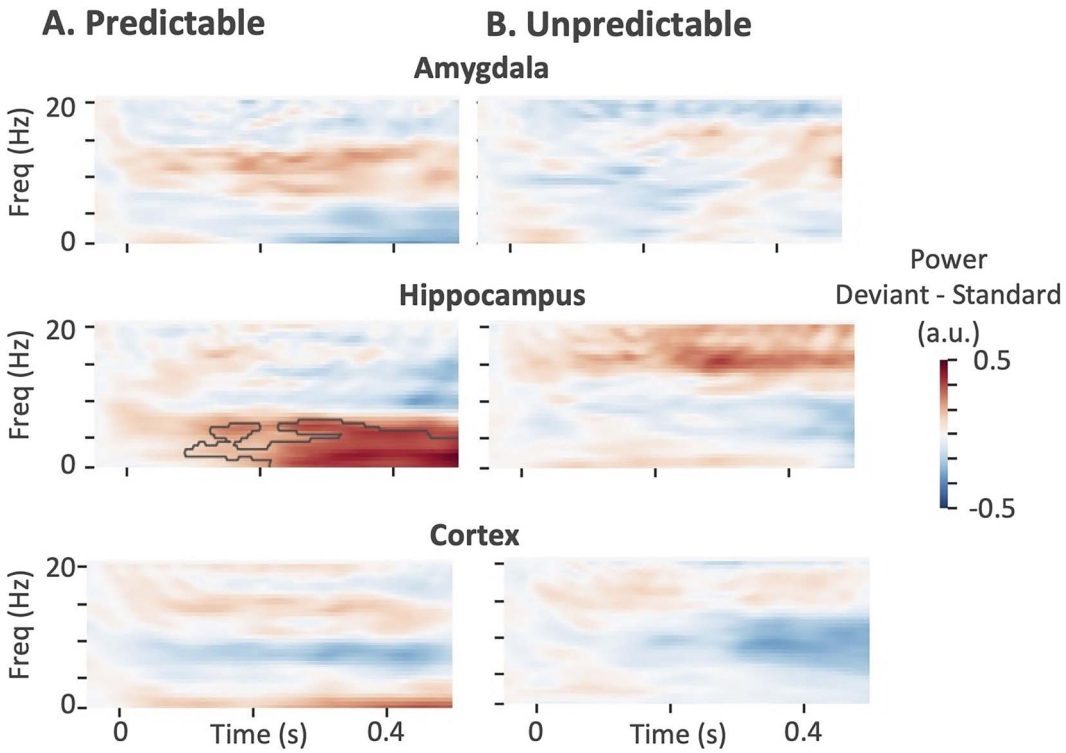


**Fig. 7.** Deviant–standard power across patients and regions. Each plot illustrates the difference in average power in response to deviant–standard sounds, for the predictable (A) and unpredictable (B) contexts. A significant increase in low-frequency power was observed for the predictable context only for the hippocampus (cluster-level $P_{corr} < 0.05$).

electrodes of the temporal cortex, studied via electrocorticography in a different patient cohort. Other studies have reported predictability effects in the temporal cortex (Chenu et al. 2013; Auksztulewicz et al. 2018; Lecaignard et al. 2022), but using different experimental protocols, where predictions were induced either via preceding visual context (Auksztulewicz et al. 2018), via the so-called local–global deviance paradigm (Chenu et al. 2013), or quantified as trial-to-trial variations (Lecaignard et al. 2022). The lack of predictability effect in our results may be due to the fact that we assessed deviance and predictability effects at the group level, across patients and electrodes, to keep consistency with previous work using a similar design (Dürschmid et al. 2016). Although sensitive, this approach is also prone to only reveal effects that are highly consistent and in the same direction across electrodes. Future studies can assess more fine-grained correlates of deviance effects in the auditory cortex, by identifying single electrode effects, as auditory predictions may manifest in spatially fine-grained cortical patterns.

Importantly, our findings suggest that the amygdala is mainly sensitive to unexpected deviance, as indicated by a higher number of contacts showing deviance effects for an unpredictable compared with predictable context and a stronger overall deviance effect (Fig. 5). Although this was the case when considering the time-course of LF-ERPs, we did not find evidence for differential power in isolated frequency bands in the amygdala when performing a time–frequency analysis, which suggests that deviance effects in the amygdala are not frequency-specific. These findings reinforce the role of the amygdala as a novelty detector (Blackford et al. 2010), or as being sensitive to events of high saliency (Fedele et al. 2020), which could be particularly relevant for cases of unpredictable deviance, as an unexpected change in the environmental statistics might signal danger (Balderston et al. 2013).

The sensitivity of the hippocampus to violations of sequences has been mainly examined in the context of active "oddball" paradigms, in the auditory (Ioannides et al. 1995) or somatosensory (Hamada et al. 2004) modalities, where participants are asked to actively detect rare target stimuli in a stream of regularly repeated events. Our finding that the hippocampus is mainly sensitive to predictable deviant sounds fits with findings of previous studies which have shown hippocampal sensitivity to violations of predicted events. In the visual modality, the hippocampus has been found to be responsive to violations of an established sequence of events, rather than completely novel events (Kumaran and Maguire 2006; Chen et al. 2013). Garrido et al. (2015) used a visual sequence of four objects, presented in a fixed, mismatch, and unpredictable order in an MEG study. Using source reconstruction techniques, these authors reported a higher theta power in the mismatch compared with the fixed or unpredictable conditions. Similar findings have also been reported in the auditory modality (Recasens et al. 2018), with additional evidence that hippocampal-to-cortical connectivity underlies the encoding of predictable sequences. The hippocampus, auditory cortex, and inferior frontal gyrus have been shown to differentiate predictable vs. random auditory sequences in an MEG study (Barascud et al. 2016). Additionally, fMRI studies have shown that the hippocampus is sensitive to visual regularities and predictions (Schapiro et al. 2012) and to the temporal distance of regularities (Ekman et al. 2023). These results are in accord with our findings, as we show a significant increase in low-frequency hippocampal power in response to predictable but not unpredictable violations of expected auditory events, and sensitivity of the hippocampus to predictable auditory sequences which unfold over time. The temporal extent of this unfolding, or how the hippocampus would track auditory sequences over longer timescales and

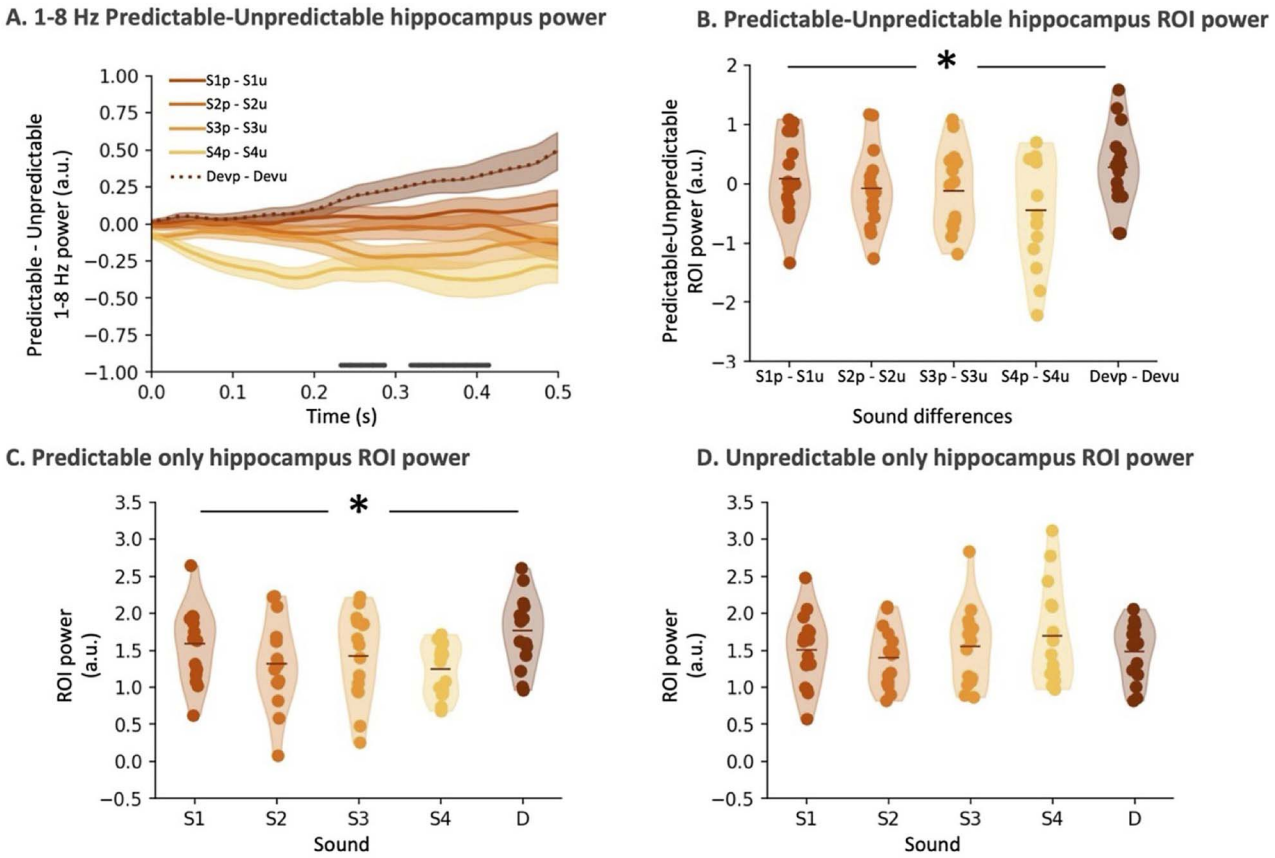


**Fig. 8.** Low-frequency difference in power in the hippocampus for predictable vs. unpredictable context as the auditory sequence unfolds. (A) Full lines illustrate mean 1–8 Hz difference in power in response to standard sounds, by order of presentation (S1–S4), subtracting power in response to predictable from unpredictable sounds. Dashed lines show 1–8 Hz power for deviant predictable minus unpredictable sounds. Horizontal lines highlight periods where the ordering was significant ($P < 0.05$). (B) Mean power in the hippocampus, computed within the ROI identified in the analysis of Fig. 7, as the auditory sequence unfolds, for the predictable minus unpredictable context. The mean power was computed for each contact via the mask of significant deviance effects in hippocampus (Fig. 7) and showed a significant effect of sequence ($F(1,14) = 7.87$, $P_{corr} < 0.05$). (C and D) Mean power masked by deviance effects for the predictable (C) and unpredictable contexts (D) separately. Only the predictable context showed a significant effect of sequence ($F(1,14) = 8.29$, $P_{corr} < 0.05$). S1-4p: Standard first, predictable; S1-4u: Standard 1–4, unpredictable. Devp: Deviant predictable, Devu: Deviant unpredictable.

longer sequences remain open questions. Although we cannot fully exclude that some of our effects of power changes in the hippocampus as the auditory sequence unfolds may be due to the acoustic characteristics of the deviant sounds, these were similar for the predictable and unpredictable context. However, the different effects we observed for the two contexts in the hippocampus suggest that any effects due to the sounds' physical characteristics are negligible.

Overall, our findings suggest that low-frequency hippocampal activity contributes to the detection of auditory sequences and formation of auditory predictions. Low-frequency activity in the hippocampus has been previously shown to mediate working memory (Johnson et al. 2018; Boran et al. 2019), information flow from and to auditory cortex (Dimakopoulos et al. 2022), and predictions of future events (Sherman and Turk-Browne 2020). Our results expand the functions of low-frequency hippocampal activity toward a role in maintaining an active model of environmental regularities. We found that the difference in hippocampal low-frequency power between standard and deviant sounds increases the closer a sequence gets to a deviant sound, but only when the occurrence of a deviant sound can be predicted (Fig. 8). One interpretation for these findings is that the hippocampus plays an active role in updating an environmental model, keeping track of an ongoing sequence as it rapidly evolves across a sequence of auditory events. Similar findings have been reported for the prefrontal cortex, which has also been shown to be sensitive to ongoing auditory sequences (Dürschmid et al. 2018). Whether this tracking of auditory patterns is an inherent property of the hippocampus, or driven by external input, such as the prefrontal cortex, remains to be investigated.

## Limitations and future directions

One main limitation of our study is the sparse electrode coverage: because our primary goal was to investigate hippocampal and amygdala contributions in deviance detection and auditory predictions, we focused on patients that had good coverage in the medial temporal lobe, with at least one hemisphere being seizure-free. As a consequence, in our patient cohort, there were no patients with frontal depth electrodes or grids, which would have allowed investigation of hippocampal–amygdalo–prefrontal interactions. Future studies can profit from recent advances of high-precision MEG to reconstruct medial temporal lobe activity (Tzovara et al. 2019) and study how the medial temporal lobe network interacts with prefrontal regions. Another limitation of our study is that because of the tight timing in our experimental setup, we were not able to assess metrics of functional connectivity among our three target regions, which typically rely on

oscillatory coupling, that evolves over longer temporal intervals (Dimakopoulos et al. 2022; Li, Cao, Yu, Xiao, et al. 2023; Li, Cao, Yu, Wang, et al. 2023). Our findings on the timing of onsets and peaks auditory responses and deviance effects provide a first indication on the information flow in the amygdalo-hippocampal-temporal network that can be confirmed using longer sound intervals. Future work can also evaluate the extent to which our results are driven by differences in the acoustic characteristics between standard and deviant sounds. Although we cannot fully exclude that some of our effects that we found, for example, relating to power changes in the hippocampus as the auditory sequence unfolds may be due to the acoustic characteristics of the deviant sounds, these were similar for the predictable and unpredictable context. The different effects observed for these two contexts at least in the hippocampus and amygdala lead us to believe that any effects due to the sounds' physical characteristics are negligible. Last, the present design cannot answer the question of whether the hippocampus and amygdala are performing computations related to deviance detection and predictions or whether they rely on computations from other brain regions. Future studies with causal interventions could shed light into that question.

## Conclusions

We provide evidence for the existence of an extended temporal lobe network underlying auditory predictions. Our findings complement existing studies that have focused on the cortex and suggest that the search for sensory predictions and prediction error signals needs extension to medial temporal regions. Importantly, our findings suggest the existence of a distributed network underlying the generation of auditory predictions, comprising cortical sensory areas, which compute a "low"-level prediction, the amygdala, which is sensitive to unexpected violations of streams of sensory information, and the hippocampus, which computes auditory predictions through low-frequency activity.

## Author contributions

AT: Conceptualization, Formal Analysis, Funding acquisition, Visualization, Writing - original draft; TF: Methodology, Investigation, Data curation; JS: Methodology, Investigation, Data curation, Resources; DL: Investigation, Data curation; JJL: Investigation, Methodology; RTK: Conceptualization, Funding acquisition, Resources, Supervision, Writing - original draft. All authors: Writing - review & editing.

## Supplementary material

Supplementary material is available at *Cerebral Cortex* online.

## Funding

This work was supported by the Interfaculty Research Cooperation "Decoding Sleep: From Neurons to Health & Mind" of the University of Bern (to AT), the Swiss National Science Foundation (grant numbers 320030_188737, P300PA_174451 to AT),. RTK is supported by NINDS RONS21135 and NIMH CONTE Center PO-MH109429. RTK and JJL is supported by the Brain Initiative U19 NS1076 and U01NS108916.

*Conflict of interest statement:* None declared.

## References

Auksztulewicz R, Schwiedrzik CM, Thesen T, Doyle W, Devinsky O, Nobre AC, Schroeder CE, Friston KJ, Melloni L. Not all predictions are equal: "what" and "when" predictions modulate activity in auditory cortex through different mechanisms. *J Neurosci*. 2018:38(40):8680–8693. https://doi.org/10.1523/JNEUROSCI.0369-18.2018.

Axmacher N, Cohen MX, Fell J, Haupt S, Dümpelmann M, Elger CE, Schlaepfer TE, Lenartz D, Sturm V, Ranganath C. Intracranial EEG correlates of expectancy and memory formation in the human hippocampus and nucleus accumbens. *Neuron*. 2010:65(4):541–549. https://doi.org/10.1016/j.neuron.2010.02.006.

Balderston NL, Schultz DH, Helmstetter FJ. The effect of threat on novelty evoked amygdala responses. *PLoS One*. 2013:8(5):e63220. https://doi.org/10.1371/journal.pone.0063220.

Bar M. Predictions: a universal principle in the operation of the human brain. Introduction. *Philos Trans R Soc Lond Ser B Biol Sci*. 2009:364(1521):1181–1182. https://doi.org/10.1098/rstb.2008.0321.

Barascud N, Pearce MT, Griffiths TD, Friston KJ, Chait M. Brain responses in humans reveal ideal observer-like sensitivity to complex acoustic patterns. *Proc Natl Acad Sci U S A*. 2016:113(5):E616–E625. https://doi.org/10.1073/pnas.1508523113.

Blackford JU, Buckholtz JW, Avery SN, Zald DH. A unique role for the human amygdala in novelty detection. *NeuroImage*. 2010:50(3):1188–1193. https://doi.org/10.1016/j.neuroimage.2009.12.083.

Blenkmann AO, Collavini S, Lubell J, Llorens A, Funderud I, Ivanovic J, Pål G. Larsson, et al. Auditory deviance detection in the human insula: an intracranial EEG study. *Cortex*. 2019:1:189–200. https://doi.org/10.1016/j.cortex.2019.09.002.

Boran E, Fedele T, Klaver P, Hilfiker P, Stieglitz L, Grunwald T, Sarnthein J. Persistent hippocampal neural firing and hippocampal-cortical coupling predict verbal working memory load. *Sci Adv*. 2019:5(3):eaav3687. https://doi.org/10.1126/sciadv.aav3687.

Camalier CR, Scarim K, Mishkin M, Averbeck BB. A comparison of auditory oddball responses in dorsolateral prefrontal cortex, basolateral amygdala, and auditory cortex of macaque. *J Cogn Neurosci*. 2019:31(7):1054–1064. https://doi.org/10.1162/jocn_a_01387.

Canolty RTT, Edwards E, Dalal SS, Soltani M, Nagarajan SS, Kirsch HE, Berger MS, Barbaro NM, Knight RT. High gamma power is phase-locked to theta oscillations in human neocortex. *Science (New York, N.Y.)* 2006:313(5793):1626–1628. https://doi.org/10.1126/science.1128115.

Chen J, Dastjerdi M, Foster BL, LaRocque KF, Rauschecker AM, Parvizi J, Wagner AD. Human hippocampal increases in low-frequency power during associative prediction violations. *Neuropsychologia*. 2013:51(12):2344–2351. https://doi.org/10.1016/j.neuropsychologia.2013.03.019.

Chennu S, Noreika V, Gueorguiev D, Blenkmann A, Kochen S, Ibáñez A, Owen AM, Tristan a Bekinschtein. Expectation and attention in hierarchical auditory prediction. *J Neurosci*. 2013:33(27):11194–11205. https://doi.org/10.1523/JNEUROSCI.0114-13.2013.

Cusinato R, Alnes SL, van Maren E, Boccalaro I, Ledergerber D, Adamantidis A, Imbach LL, Schindler K, Baud MO, Tzovara A. Intrinsic neural timescales in the temporal lobe support an auditory processing hierarchy. *Journal of Neuroscience*. 2023:43(20):3696–3707. https://doi.org/10.1523/JNEUROSCI.1941-22.2023.

Dimakopoulos V, Mégevand P, Stieglitz LH, Imbach L, Sarnthein J. Information flows from hippocampus to auditory cortex during replay of verbal working memory items. *elife*. 2022:11(August):e78677. https://doi.org/10.7554/eLife.78677.

Dürschmid S, Edwards E, Reichert C, Dewar C, Hinrichs H, Heinze H-J, Kirsch HE, Dalal SS, Deouell LY, Knight RT. Hierarchy of prediction errors for auditory events in human temporal and frontal cortex. *Proc Natl Acad Sci*. 2016:113(24):201525030–201526760. https://doi.org/10.1073/pnas.1525030113.

Dürschmid S, Zaehle T, Hinrichs H, Heinze HJ, Voges J, Garrido MI, Dolan RJ, Knight RT. Sensory deviancy detection measured directly within the human nucleus accumbens. *Cereb Cortex*. 2016:26(3):1168–1175. https://doi.org/10.1093/cercor/bhu304.

Dürschmid S, Reichert C, Hinrichs H, Heinze H-J, Kirsch HE, Knight RT, Knight RT, Deouell LY. Direct evidence for prediction signals in frontal cortex independent of prediction error. *Cereb Cortex*. 2018:29(11):4530–4538. https://doi.org/10.1093/cercor/bhy331.

Edwards E, Soltani M, Deouell LY, Berger MS, Knight RT. High gamma activity in response to deviant auditory stimuli recorded directly from human cortex. *J Neurophysiol*. 2005:94(6):4269–4280. https://doi.org/10.1152/jn.00324.2005.

Eichenbaum H. Memory on time. *Trends Cogn Sci*. 2013:17(2):81–88. https://doi.org/10.1016/j.tics.2012.12.007.

Ekman M, Kusch S, De Lange F. Successor-like representation guides the prediction of future events in human visual cortex and hippocampus. *elife*. 2023:12. https://doi.org/10.7554/eLife.78904.

Fedele T, Tzovara A, Steiger B, Hilfiker P, Grunwald T, Stieglitz L, Jokeit H, Sarnthein J. The relation between neuronal firing, local field potentials and hemodynamic activity in the human amygdala in response to aversive dynamic visual stimuli. *NeuroImage*. 2020:213:116705. https://doi.org/10.1016/j.neuroimage.2020.116705.

Garrido MI, Friston KJ, Kiebel SJ, Stephan KE, Baldeweg T, Kilner JM. The functional anatomy of the MMN: a DCM study of the roving paradigm. *NeuroImage*. 2008:42(2):936–944. https://doi.org/10.1016/j.neuroimage.2008.05.018.

Garrido MI, Kilner JM, Stephan KE, Friston KJ. The mismatch negativity: a review of underlying mechanisms. *Clin Neurophysiol*. 2009:120(3):453–463. https://doi.org/10.1016/j.clinph.2008.11.029.

Garrido MI, Barnes GR, Kumaran D, Maguire EA, Dolan RJ. Ventromedial prefrontal cortex drives hippocampal theta oscillations induced by mismatch computations. *NeuroImage*. 2015:120:362–370. https://doi.org/10.1016/j.neuroimage.2015.07.016.

Gramfort A, Luessi M, Larson E, Engemann DA, Strohmeier D, Brodbeck C, Goj R, Jas M, Brooks T, Parkkonen L, Hämäläinen M. MEG and EEG data analysis with MNE-Python. *Frontiers in Neuroscience*. 2013:7. https://doi.org/10.3389/fnins.2013.00267.

Halgren E, Squires NK, Wilson CL, Rohrbaugh JW, Babb TL, Crandall PH. Endogenous potentials generated in the human hippocampal formation and amygdala by infrequent events. *Science*. 1980:210(4471):803–805. https://doi.org/10.1126/science.7434000.

Hamada Y, Sugino K, Kado H, Suzuki R. Magnetic fields in the human hippocampal area evoked by a somatosensory oddball task. *Hippocampus*. 2004:14(4):426–433. https://doi.org/10.1002/hipo.10196.

Heilbron M, Chait M. Great expectations: is there evidence for predictive coding in auditory cortex? *Neuroscience*. 2018:389:54–73. https://doi.org/10.1016/j.neuroscience.2017.07.061.

Ioannides AA, Liu MJ, Liu LC, Bamidis PD, Hellstrand E, Stephan KM. Magnetic field tomography of cortical and deep processes: examples of 'real-time mapping' of averaged and single trial MEG signals. *Int J Psychophysiol*. 1995:20(3):161–175. https://doi.org/10.1016/0167-8760(95)00031-3.

Jafarpour A, Piai V, Lin J, Jack, Knight Robert T. Human hippocampal pre-activation predicts behavior. *Sci Rep*. 2017:7(1):5959. https://doi.org/10.1038/s41598-017-06477-5.

James CE, Michel CM, Britz J, Vuilleumier P, Hauert CA. Rhythm evokes action: early processing of metric deviances in expressive music by experts and laymen revealed by ERP source imaging. *Hum Brain Mapp*. 2012:33(12):2751–2767. https://doi.org/10.1002/hbm.21397.

Johnson EL, Knight RT. Intracranial recordings and human memory. *Curr Opin Neurobiol*. 2015:31:18–25. https://doi.org/10.1016/j.conb.2014.07.021.

Johnson EL, Adams JN, Solbakk A-κ, Tor Endestad G, Larsson JI, Meling TR, Lin JJ, Knight RT. Dynamic frontotemporal systems process space and time in working memory. *PLoS Biol*. 2018:16(3):e2004274. https://doi.org/10.1371/journal.pbio.2004274.

Johnson E, Kam J, Tzovara A, Knight RT. Insights into human cognition from intracranial EEG: a review of audition, memory, internal cognition, and causality. *J. Neural Eng., September*. 2020:17(5):051001. https://doi.org/10.1088/1741-2552/abb7a5.

Kam JWY, Lin JJ, Solbakk AK, Endestad T, Larsson PG, Knight RT. Default network and frontoparietal control network theta connectivity supports internal attention. *Nature Human Behaviour*. 2019:3(12):1263–1270. https://doi.org/10.1038/s41562-019-0717-0.

Kam JWY, Helfrich RF, Solbakk A-K, Endestad T, Larsson PG, Lin JJ, Knight RT. Top–down attentional modulation in human frontal cortex: differential engagement during external and internal attention. *Cereb Cortex*. 2021:31(2):873–883. https://doi.org/10.1093/cercor/bhaa262.

Knight RT. Contribution of human hippocampal region to novelty detection. *Nature*. 1996:383(6597):256–259. https://doi.org/10.1038/383256a0.

Kumaran D, Maguire EA. An unexpected sequence of events: mismatch detection in the human hippocampus. *PLoS Biol*. 2006:4(12):2372–2382. https://doi.org/10.1371/journal.pbio.0040424.

Lachaux JP, Axmacher N, Mormann F, Halgren E, Crone NE. High-frequency neural activity and human cognition: Past, present and possible future of intracranial EEG research. *Progress in Neurobiology*. 2012:98(3):279–301. https://doi.org/10.1016/j.pneurobio.2012.06.008.

Lecaignard F, Bertrand O, Gimenez G, Mattout J, Caclin A. Implicit learning of predictable sound sequences modulates human brain responses at different levels of the auditory hierarchy. *Front Hum Neurosci*. 2015:9:505. https://doi.org/10.3389/fnhum.2015.00505.

Lecaignard F, Bertrand O, Caclin A, Mattout J. Neurocomputational underpinnings of expected surprise. *J Neurosci*. 2022:42(3):474–486.

Li J, Cao D, Yu S, Xiao X, Imbach L, Stieglitz L, Sarnthein J, Jiang T. Functional specialization and interaction in the amygdala-hippocampus circuit during working memory processing. *Nat Commun*. 2023:14(1):2921.

Li J, Cao D, Yu S, Wang H, Imbach L, Stieglitz L, Sarnthein J, Jiang T. Theta-alpha connectivity in the hippocampal-entorhinal circuit predicts working memory load. *J Neurosci*. 2023:JN-RM-0398-23. https://doi.org/10.1523/JNEUROSCI.0398-23.2023.

Lisman J, Redish AD. Prediction, sequences and the hippocampus. *Philos Trans R Soc Lond B Biol Sci*. 2009:364(1521):1193–1201. https://doi.org/10.1098/rstb.2008.0316.

Phillips HN, Blenkmann A, Hughes LE, Kochen S, Bekinschtein TA, Cam CAN, Rowe JB. Convergent evidence for hierarchical prediction networks from human electrocorticography and magnetoencephalography. *Cortex*. 2016:82:192–205. https://doi.org/10.1016/j.cortex.2016.05.001.

Recasens M, Gross J, Uhlhaas PJ. Low-frequency oscillatory correlates of auditory predictive processing in cortical-subcortical networks: a MEG-study. *Sci Rep*. 2018:8(1):14007. https://doi.org/10.1038/s41598-018-32385-3.

Rosburg T, Trautner P, Dietl T, Korzyukov OA, Boutros NN, Schaller C, Elger CE, Kurthen M. Subdural recordings of the mismatch negativity (MMN) in patients with focal epilepsy. *Brain*. 2005:128(4): 819–828. https://doi.org/10.1093/brain/awh442.

Schapiro AC, Kustner LV, Turk-Browne NB. Shaping of object representations in the human medial temporal lobe based on temporal regularities. *Curr Biol*. 2012:22(17):1622–1627. https://doi.org/10.1016/j.cub.2012.06.056.

Sherman BE, Turk-Browne NB. Statistical prediction of the future impairs episodic encoding of the present. *PNAS*. 2020: 117(37):22760–22770. https://doi.org/10.1073/pnas.2013291117.

Stolk A, Griffin S, Van Der Meij R, Dewar C, Saez I, Lin JJ, Piantoni G, Schoffelen JM, Knight RT, Oostenveld R. Integrated analysis of anatomical and electrophysiological human intracranial data. *Nature Protocols*. 2018:13(7):1699–1723. https://doi.org/10.1038/s41596-018-0009-6.

Tivadar RI, Knight RT, Tzovara A. Automatic sensory predictions: a review of predictive mechanisms in the brain and their link to conscious processing. *Front Hum Neurosci*. 2021:15(August):702520. https://doi.org/10.3389/fnhum.2021.702520.

Tzovara A, Meyer SS, Bonaiuto JJ, Abivardi A, Dolan RJ, Barnes GR, Bach DR. High-precision magnetoencephalography for reconstructing amygdalar and hippocampal oscillations during prediction of safety and threat. *Hum Brain Mapp*. 2019:40(14):4114–4129. https://doi.org/10.1002/hbm.24689.